Electronic Supplementary Information

A Rational Synthetic Approach to Highly Active Fe-N-C Catalyst for Efficient Electrochemical Oxygen Reduction

Sanjit Kumar Parida* Hrudananda Jena

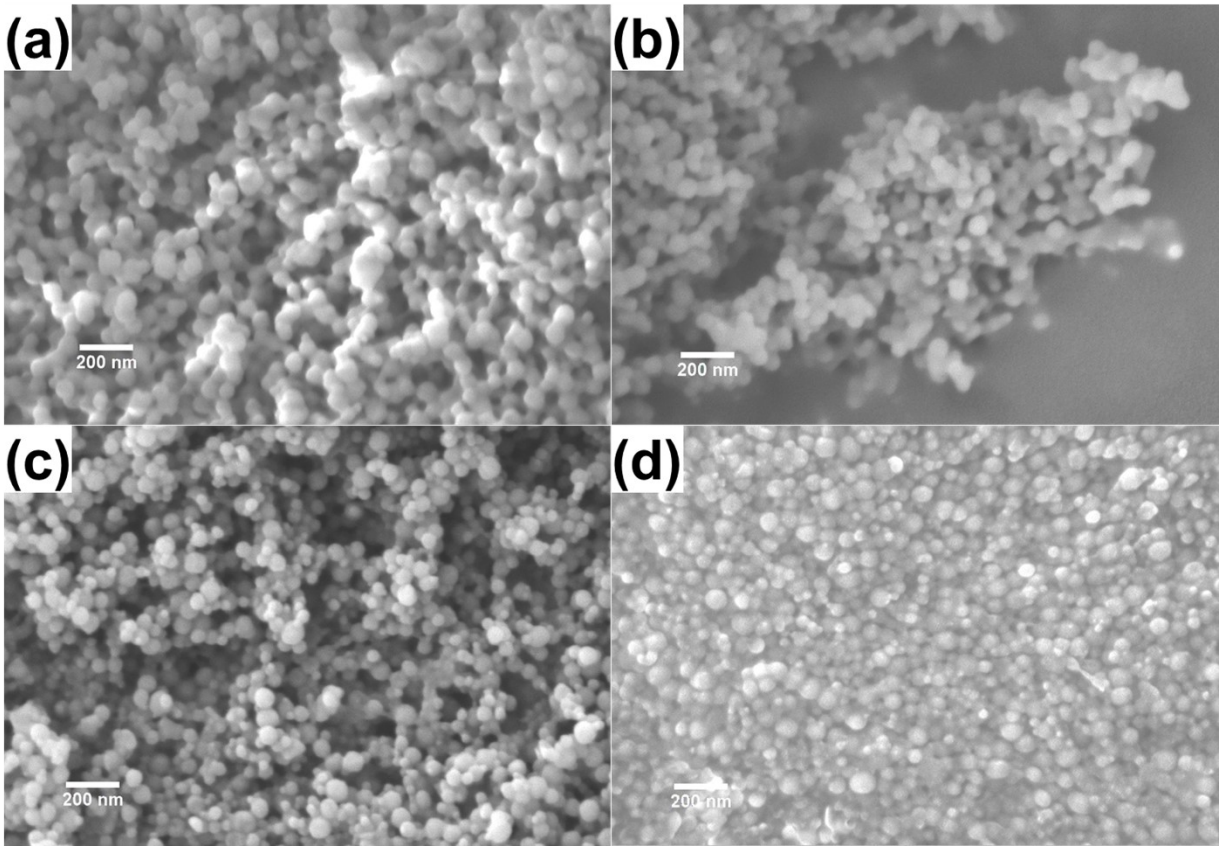

Fig. S1 FESEM images of (a) 20Fe-ZIF RT(II) (b) 20Fe-ZIF RT(III) (c) 20Fe-ZIF 70(II) and (d) 20Fe-ZIF 70(III).

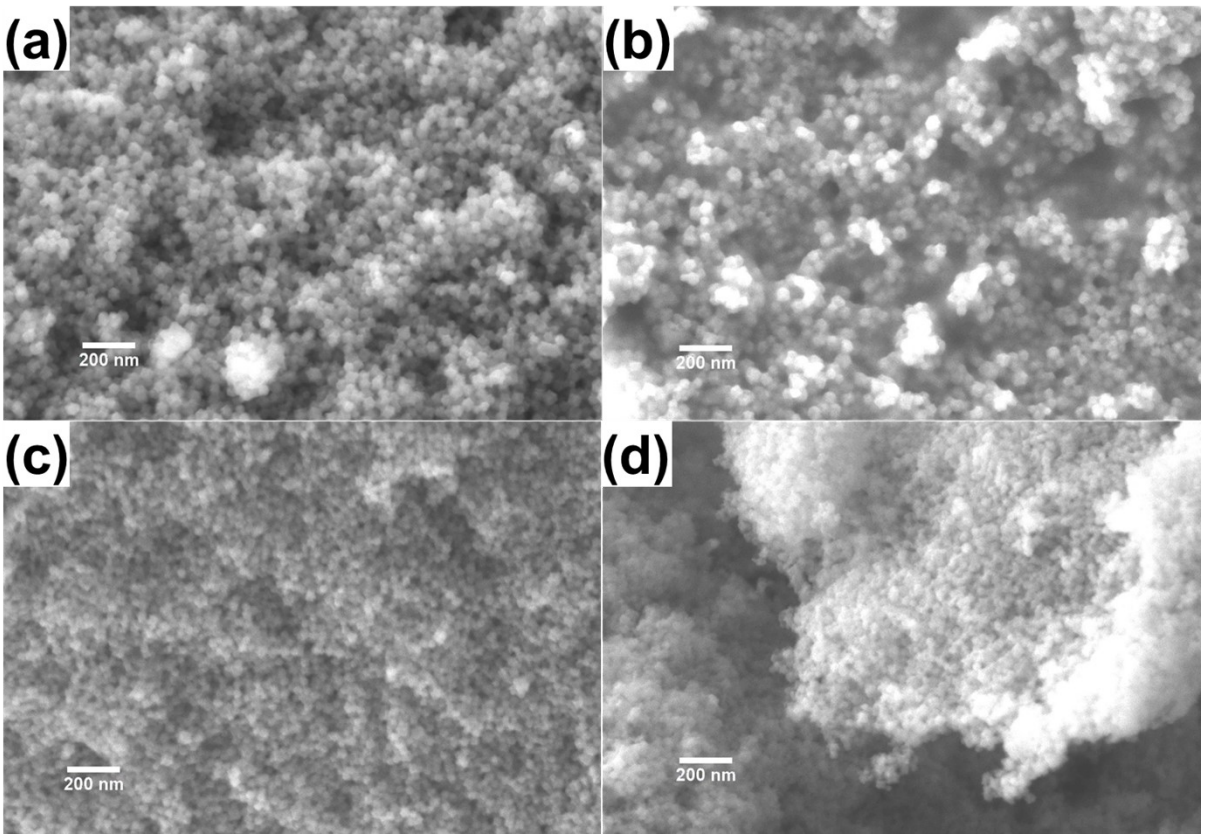

Fig. S2 FESEM images of (a) 20Fe-N-C RT(II) (b) 20Fe-N-C RT(III) (c) 20Fe-N-C 70(II) and (d) 20Fe-N-C 70(III).

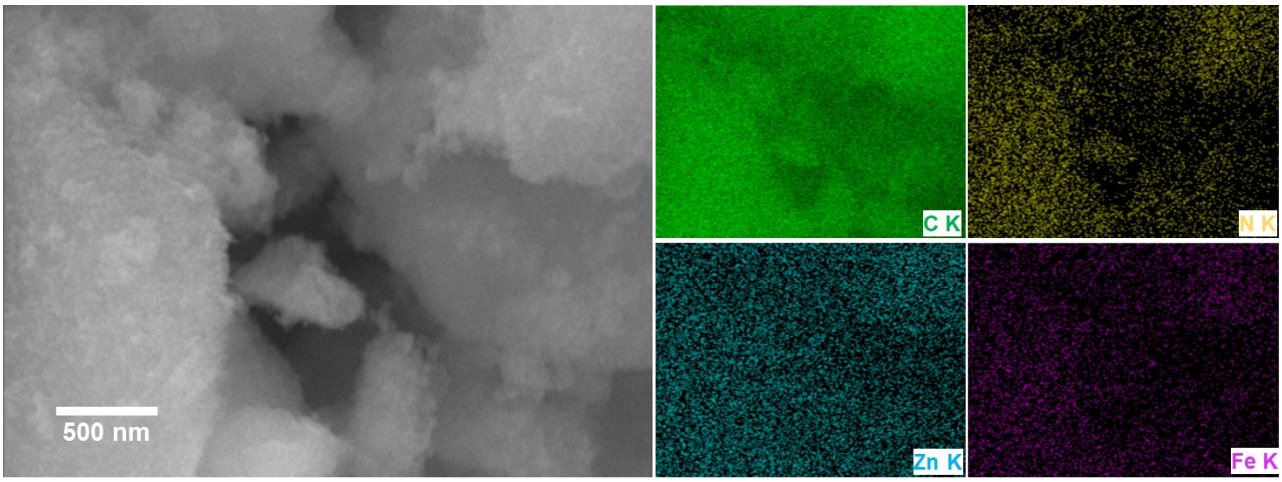

Fig. S3 (a) FESEM image, (b) Corresponding EDX elemental mapping of 20Fe-N-C RT(II).

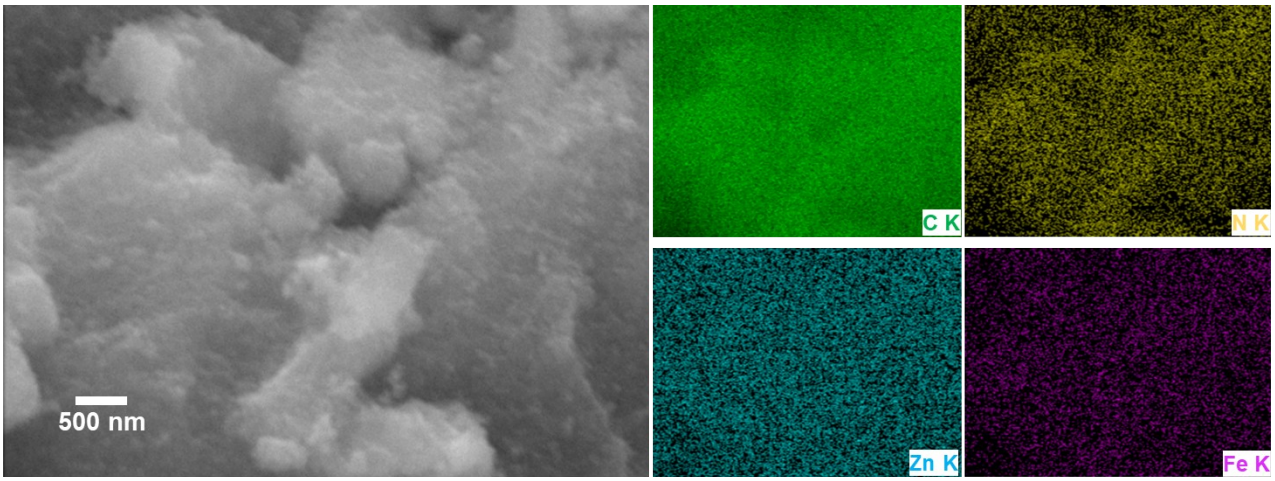

Fig. S4 (a) FESEM image, (b) Corresponding EDX elemental mapping of 20Fe-N-C RT(III).

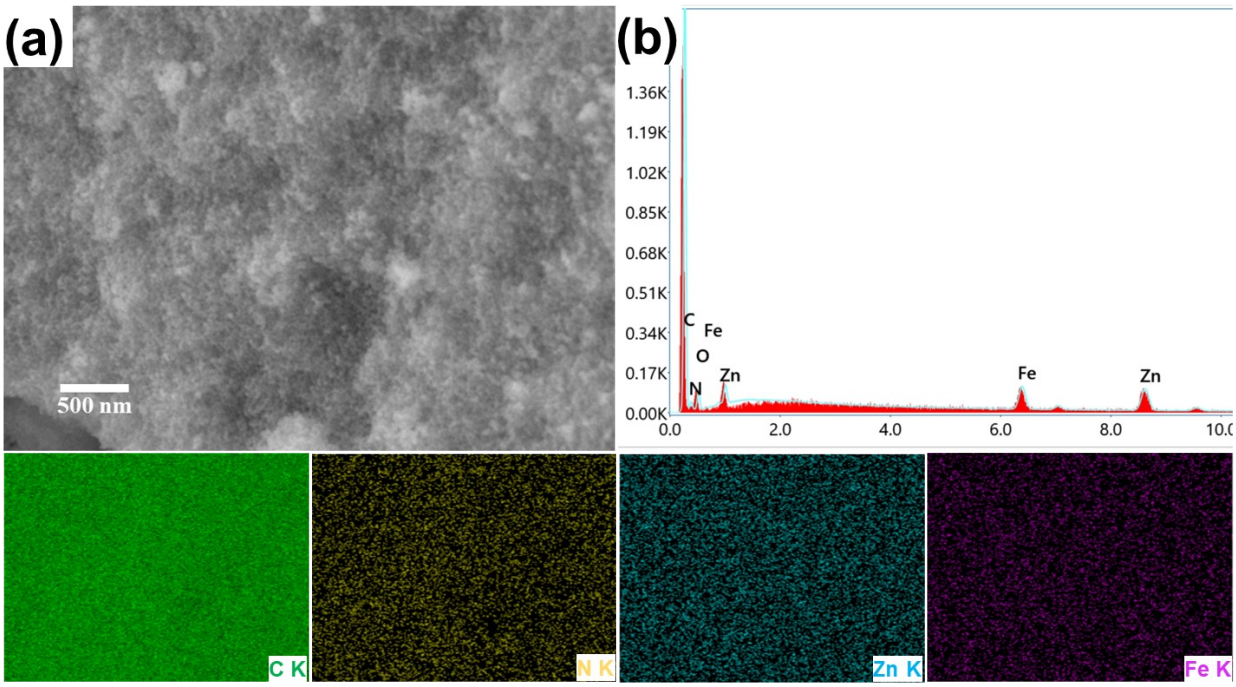

Fig. S5 (a) FESEM image, (b) EDX pattern of 20Fe-N-C-70(II) with corresponding EDX elemental mapping.

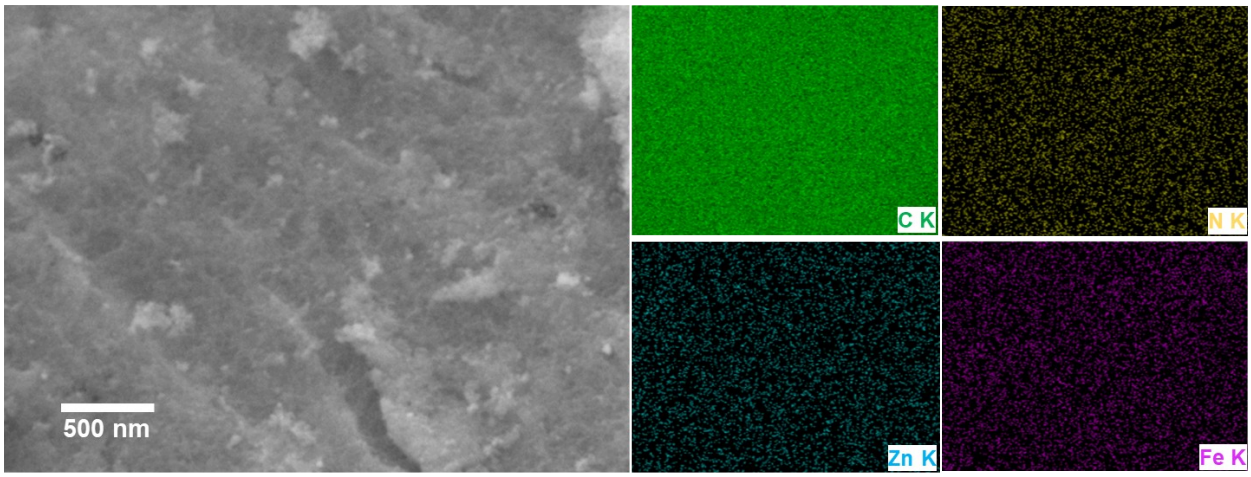

Fig. S6 (a) FESEM image, (b) Corresponding EDX elemental mapping of 20Fe-N-C 70(III).

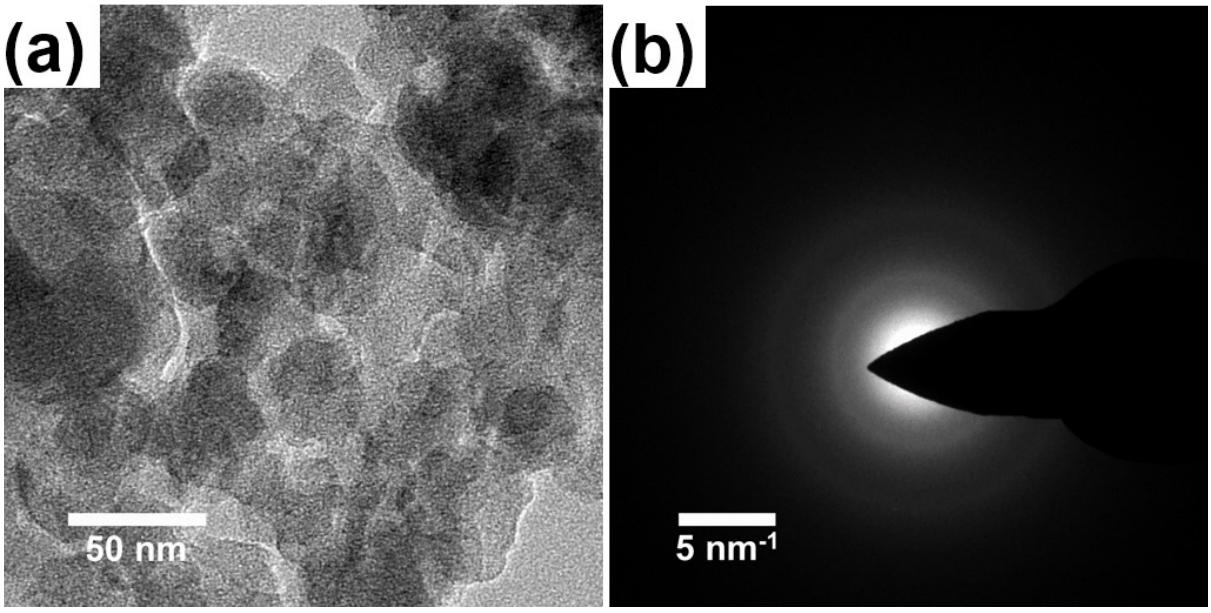

Fig. S7 (a) Representative STEM image and (b) HRTEM of 20Fe-N-C 70(II).

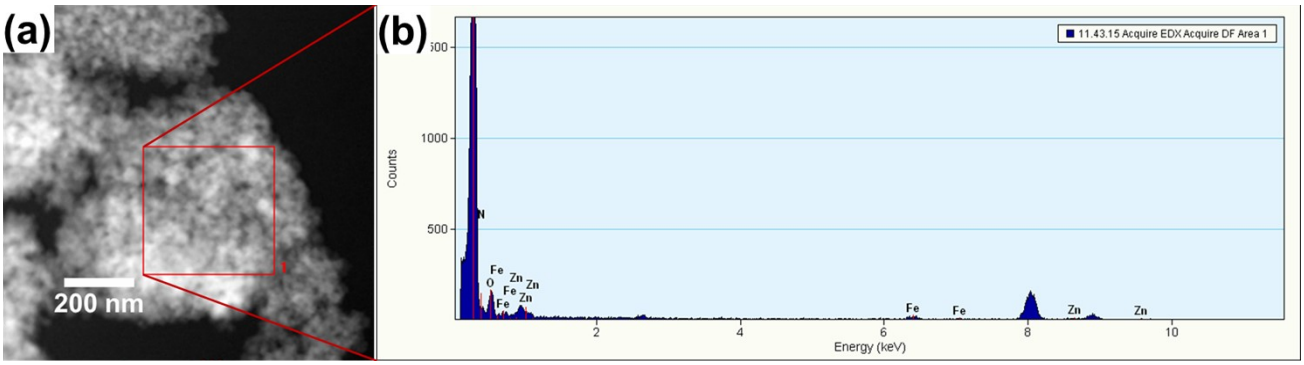

Fig. S8 (a) STEM image with (b) Corresponding EDX spectrum of 20Fe-N-C 70(II).

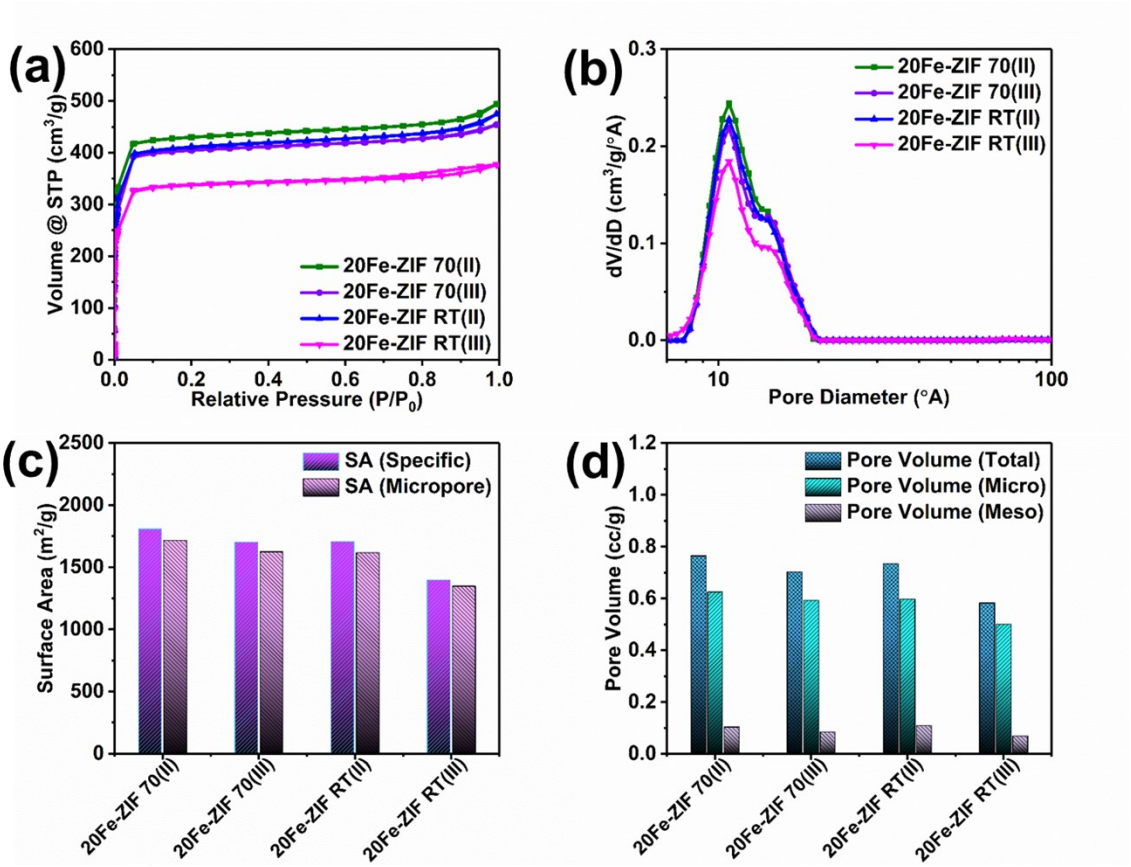

Fig. S9 (a) N_2 adsorption-desorption isotherms and (b) Pore size distribution (c) Surface area and (d) Pore volume of the 20Fe-ZIF precursors.

Table S1. BET surface area and pore size of the precursors.

Catalyst	SA_{BET} (m^2/g)	SA_{Micro} (m^2/g)	V_{Micro} (cc/g)	V_{Meso} (cc/g)	V_{Total} (cc/g)
20Fe-ZIF RT(II)	1705.7	1618.3	0.598	0.109	0.734
20Fe-ZIF RT(III)	1398.6	1349.1	0.501	0.069	0.583
20Fe-ZIF 70(II)	1807.0	1716.2	0.625	0.104	0.765
20Fe-ZIF 70(III)	1701.7	1624.9	0.593	0.085	0.703

Table S2. BET surface area and pore size of the catalysts.

Catalyst	SA_{BET} (m^2/g)	SA_{Micro} (m^2/g)	V_{Micro} (cc/g)	V_{Meso} (cc/g)	V_{Total} (cc/g)
20Fe-N-C RT(II)	1248.5	1018.4	0.424	0.221	0.730
20Fe-N-C RT(III)	1010.4	877.9	0.360	0.131	0.528
20Fe-N-C 70(II)	1337.2	1090.5	0.453	0.226	0.777
20Fe-N-C 70(III)	1135.5	937.1	0.386	0.265	0.718

Table S3. Chemical analysis results of the catalysts (ICP-OES).

Catalyst	Fe (wt.%)	Zn (wt.%)	Remark
20Fe-N-C RT(II)	1.04	0.80	
20Fe-N-C RT(III)	0.51	1.13	0.49x Fe than RT(II) sample
20Fe-N-C 70(II)	1.55	0.54	1.5x Fe than RT(II) sample
20Fe-N-C 70(III)	1.30	1.07	2.55x Fe than RT(III) sample

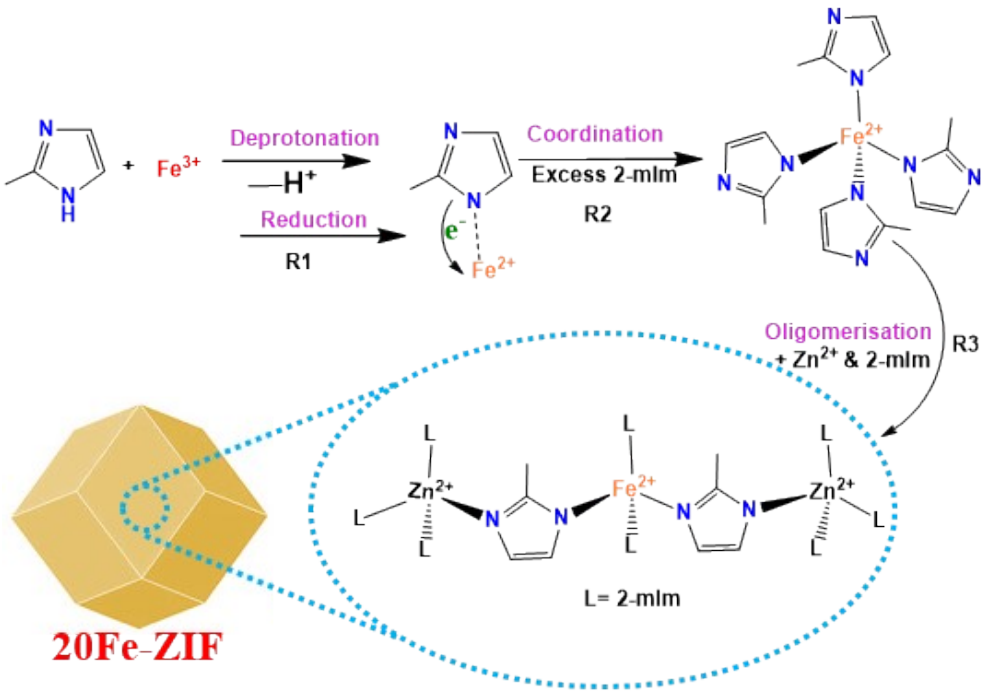

Fig. S10 Proposed mechanism of in-situ Fe^{3+} reduction during the synthesis of 20Fe-ZIF (III) precursors.

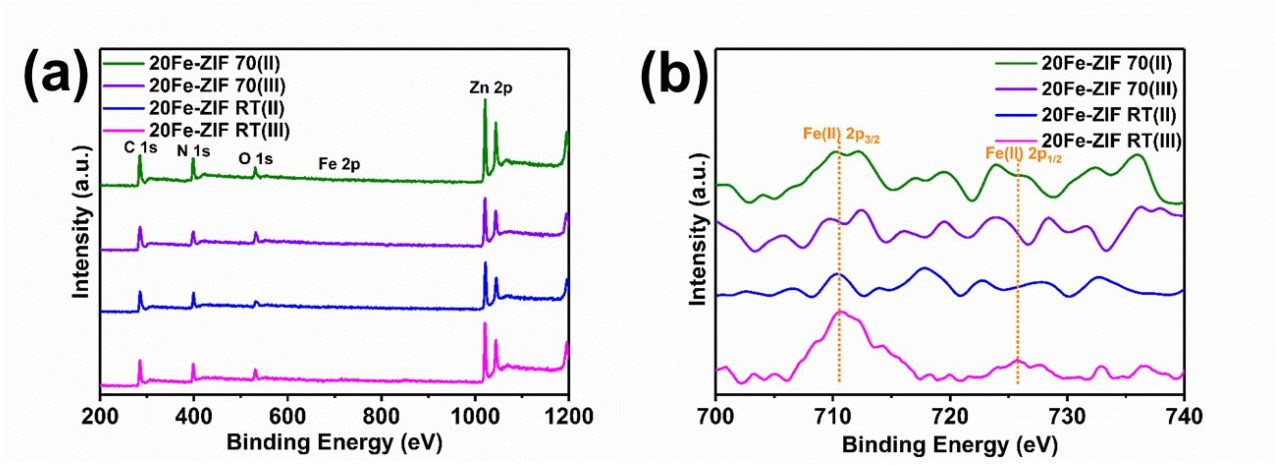

Fig. S11 (a) XPS survey spectra and (b) High resolution XPS spectra of Fe 2p in 20Fe-ZIF precursors.

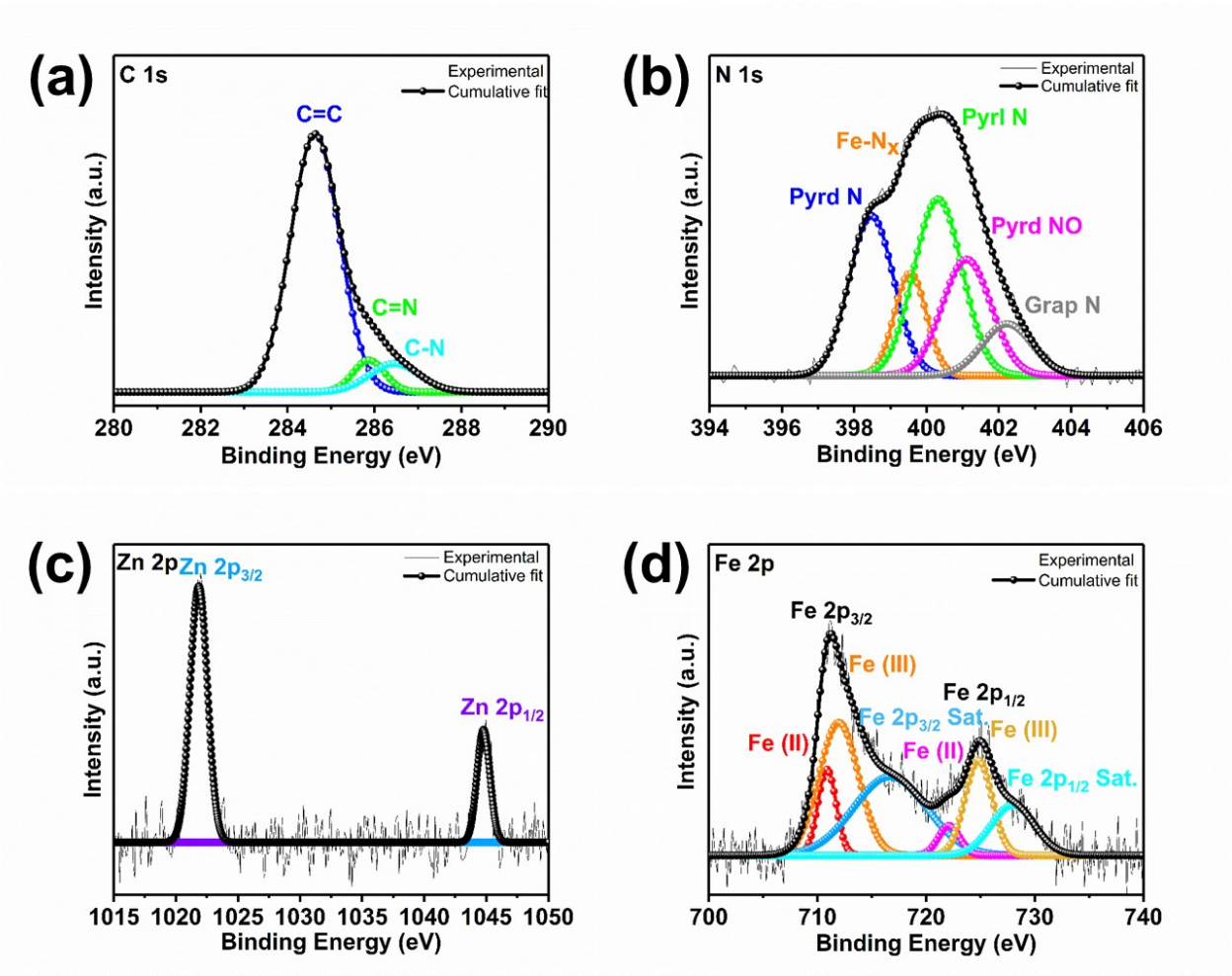

Fig. S12 High resolution XPS spectra of (a) C 1s (b) N 1s (c) Zn 2p and (d) Fe 2p in 20Fe-N-C 70(II) catalyst.

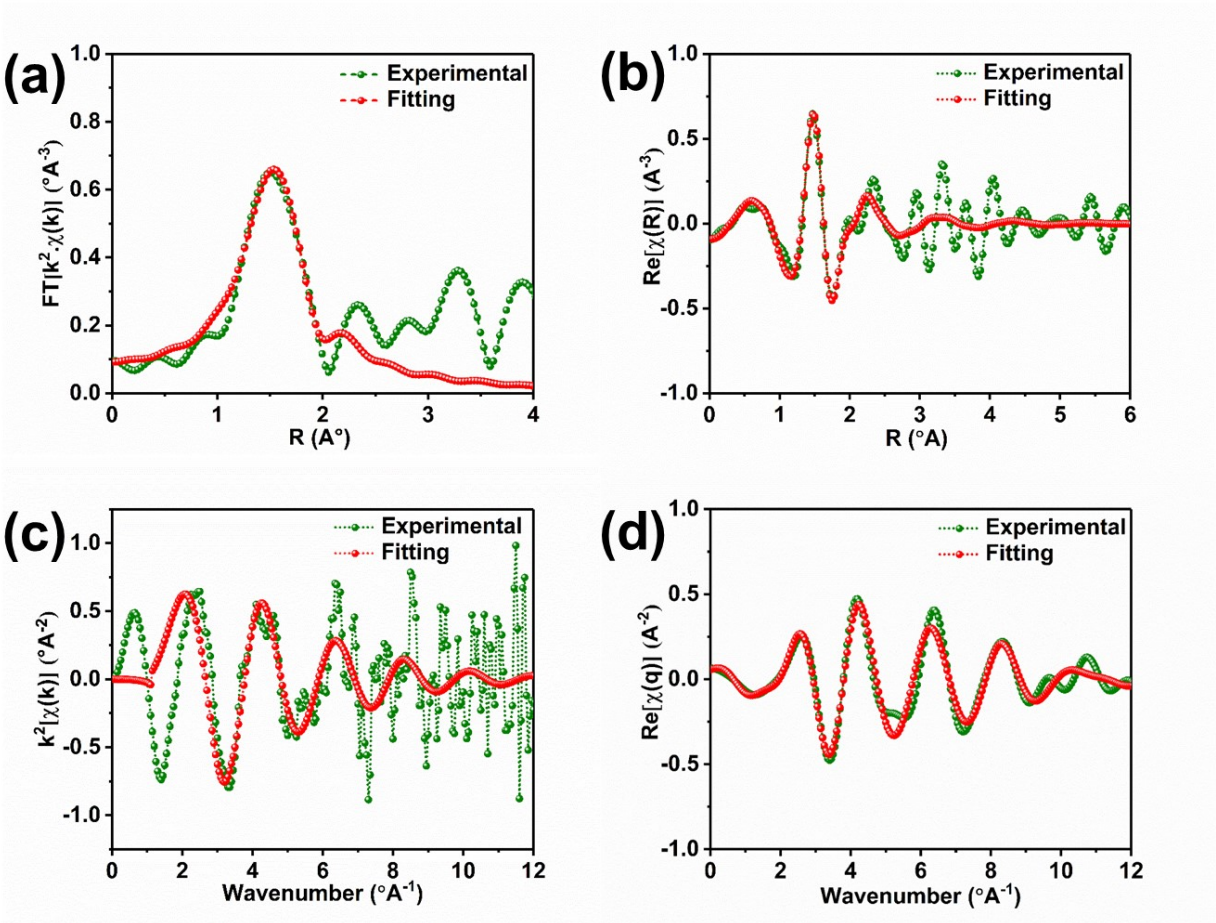

Fig. S13 Fitting results of FT-EXAFS spectra of 20Fe-N-C 70(II) in (a)-(b) R space and (c)-(d) k-space.

Table S4. Results of the fitting of the FT-EXAFS spectra collected at the Fe K-edge of 20Fe-N-C 70(II).

Sample	E_{Edge} (eV)	CN	R (°A)	σ^2	E_0 (eV)	R-factor
20Fe-N-C 70(II)	7124.48	4	1.88±0.04	0.009±0.006	4.68±1.42	0.09

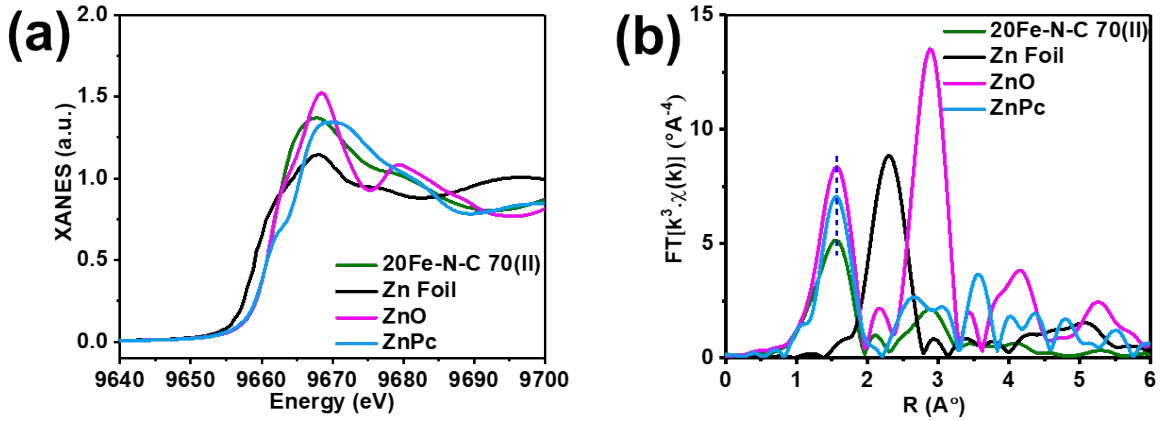

Fig. S14 (a) XANES and (b) FT-EXAFS spectra of 20Fe-N-C 70(II) and reference standards at Zn K-edge.

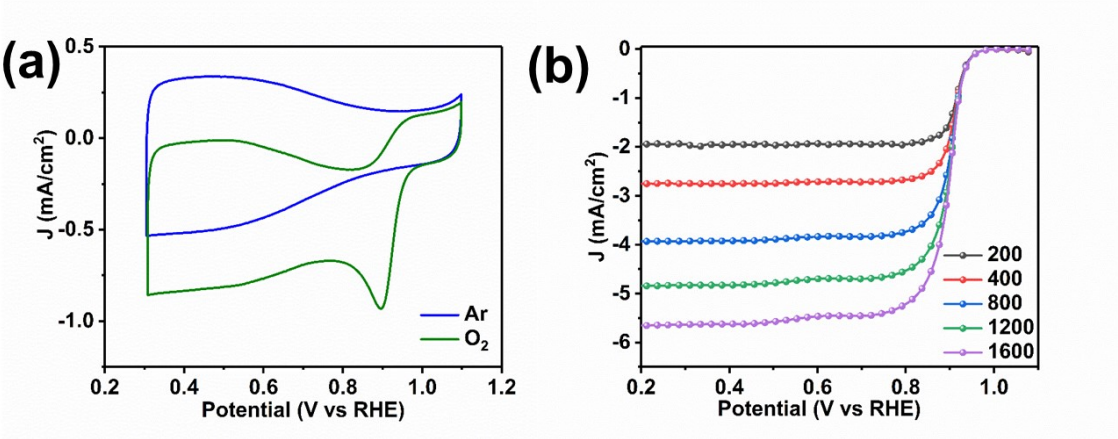

Fig. S15 (a) CV and (b) LSV curves of 20Fe-N-C RT(II) in 0.1M KOH.

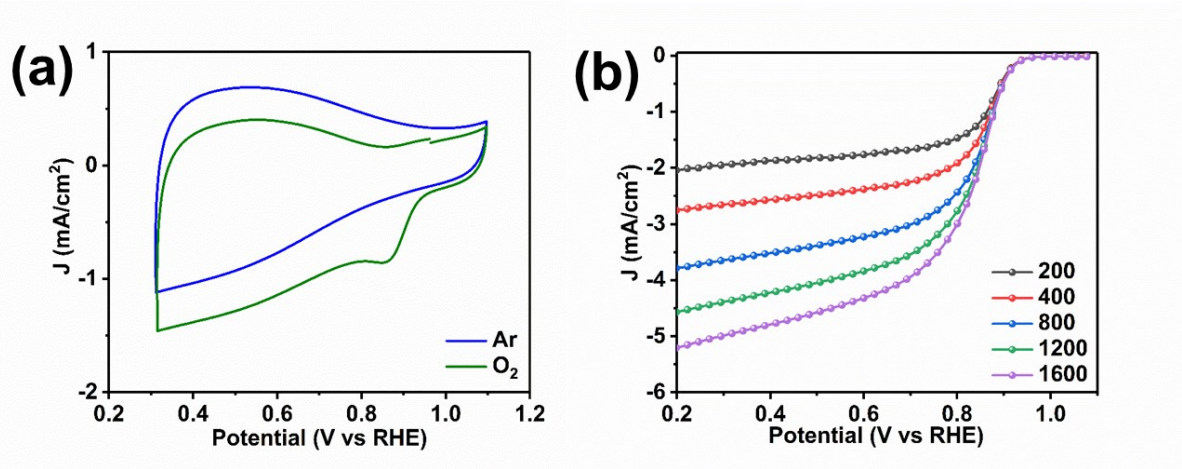

Fig. S16 (a) CV and (b) LSV curves of 20Fe-N-C RT(III) in 0.1M KOH.

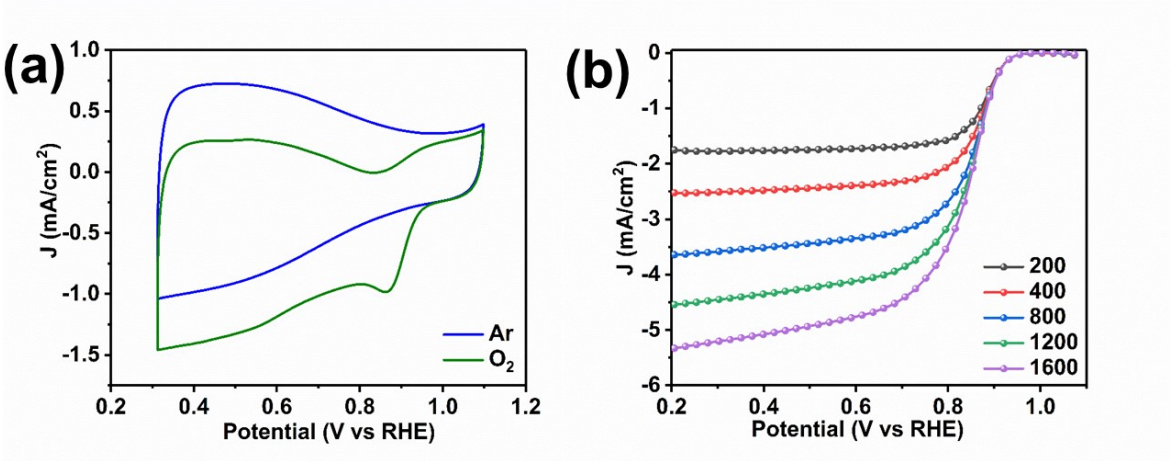

Fig. S17 (a) CV and (b) LSV curves of 20Fe-N-C 70(III) in 0.1M KOH.

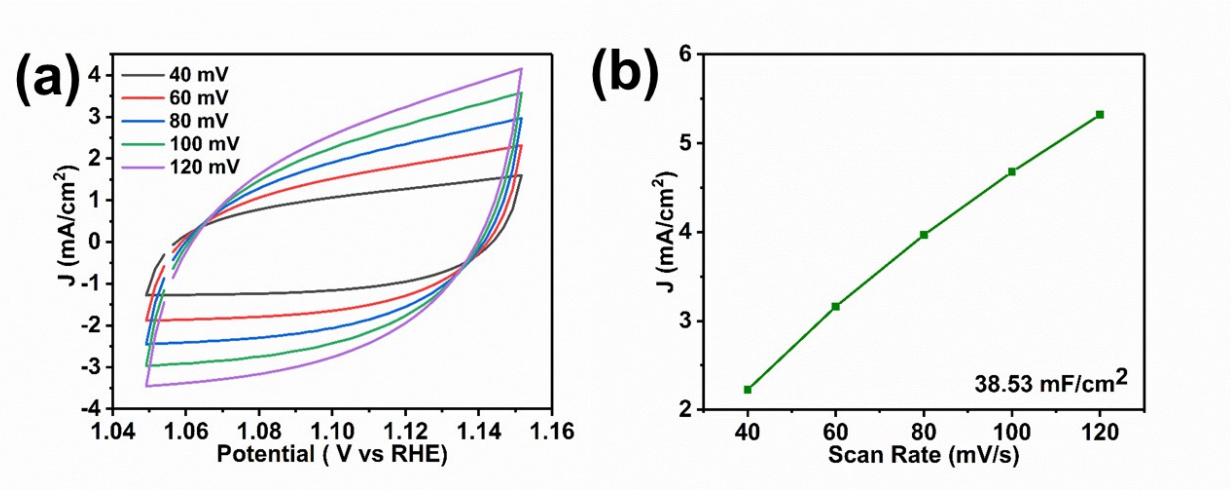

Fig. S18 Representative double-layer capacitance measurements of 20Fe-N-C 70(II) showing (a) CV curves and (b) capacitive current against the scan rates.

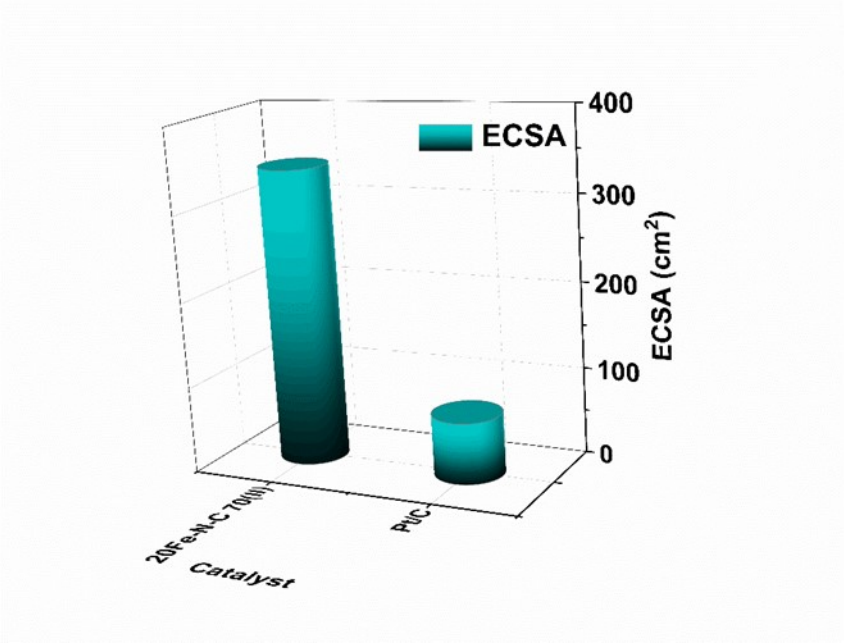

Fig. S19 Typical ECSA of the catalysts.

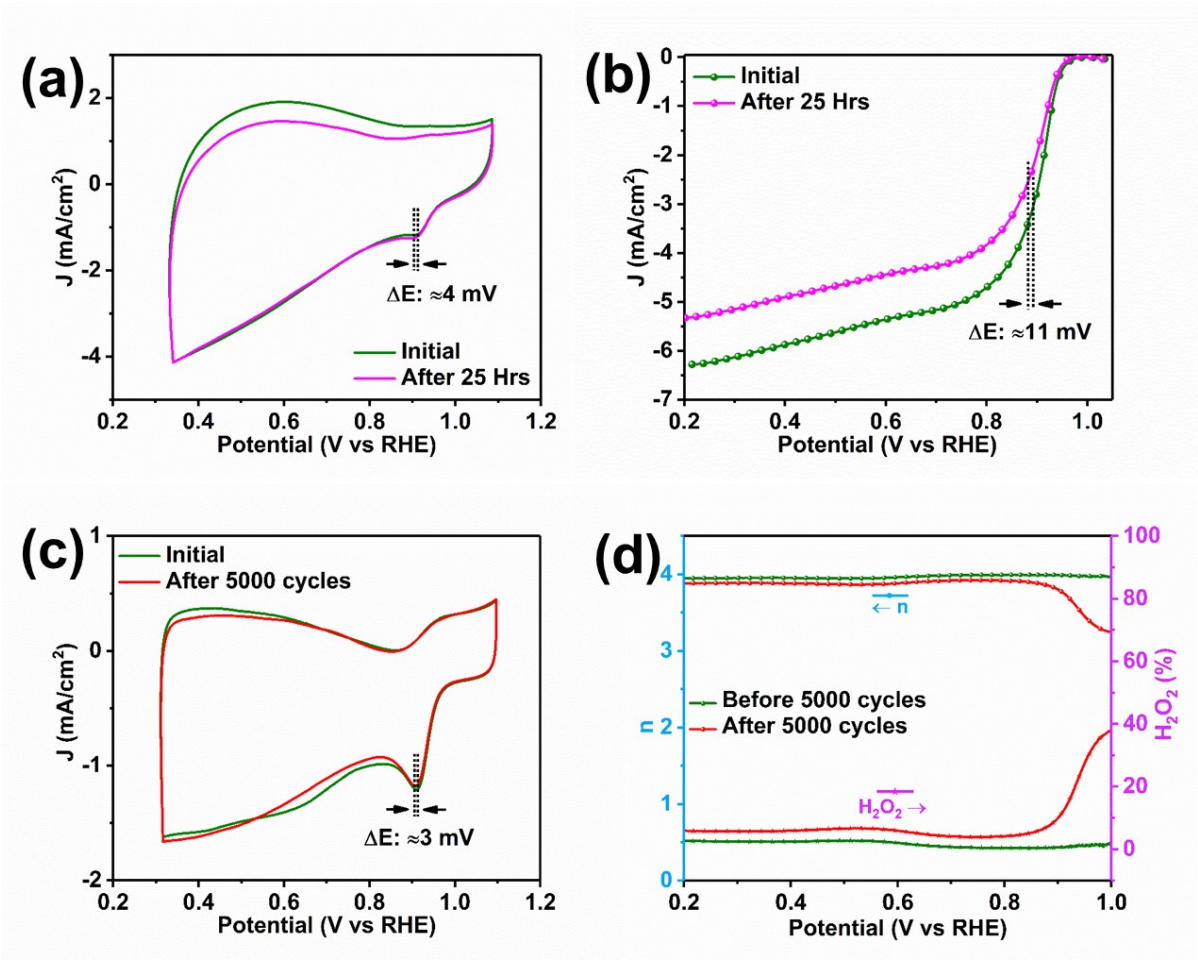

Fig. S20 (a) CV and (b) LSV curves of 20Fe-N-C 70(II) after current-time response test at 0.8V vs RHE in 0.1M KOH.

(c) CV curves and (d) RRDE results of 20Fe-N-C 70(II) before and after ADT.

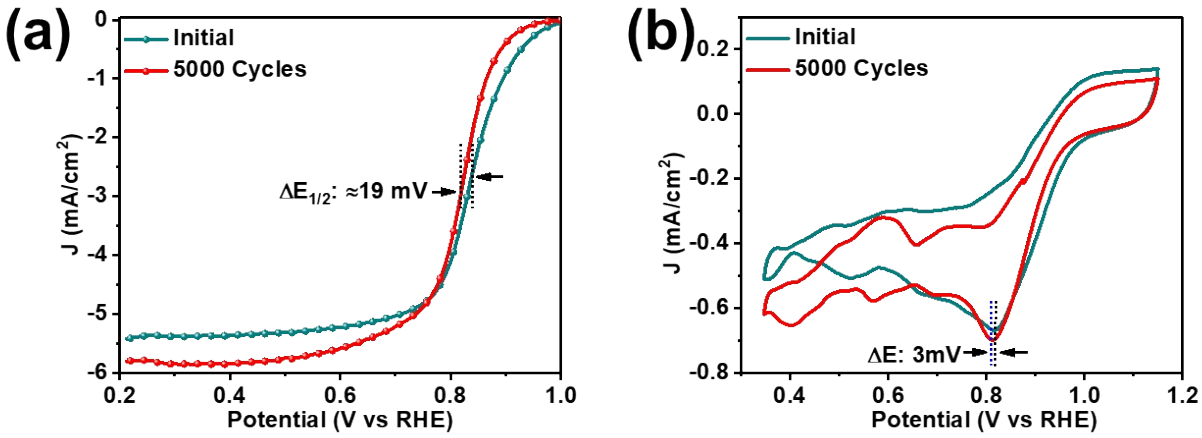

Fig. S21 (a) LSV and (b) CV curves of Pt/C before and after the accelerated stress test.

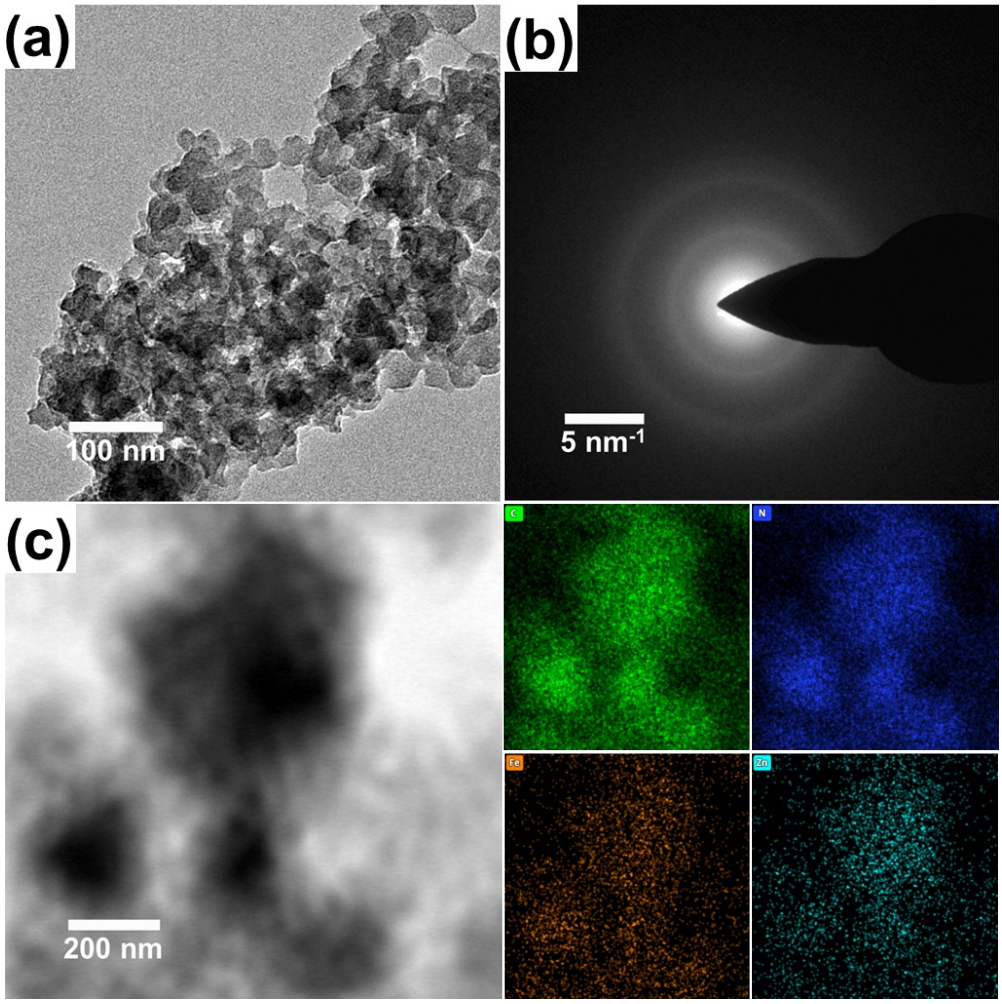

Fig. S22 (a) STEM image (b) SAED pattern (c) BF-STEM image with corresponding EDS elemental mapping result of 20Fe-N-C 70(II) after 5000 cycles of potential stress test.

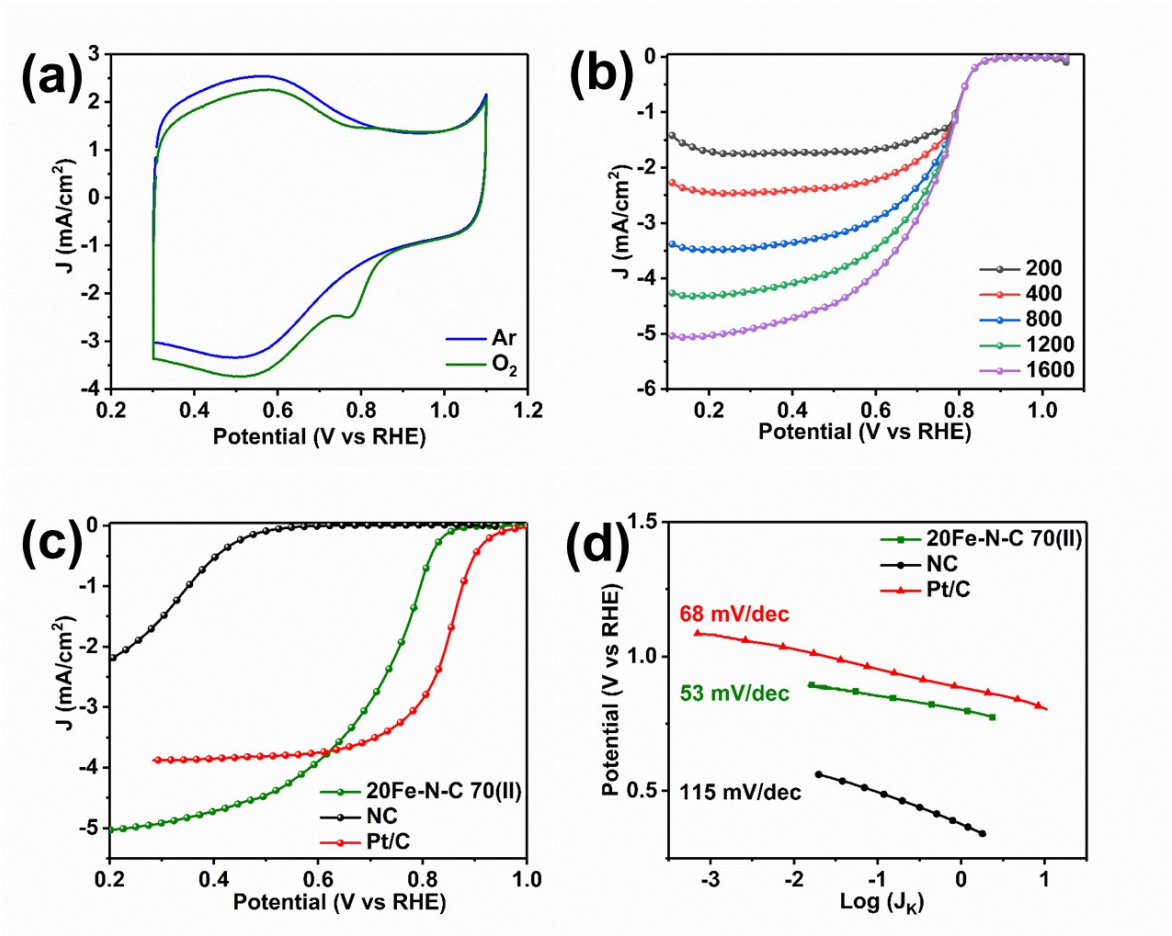

Fig. S23 (a) Electrochemical ORR activity of the catalysts in 0.5M H_2SO_4 with 800 μg/cm^2 loading showing (a) CV and (b) LSV curves of 20Fe-N-C 70(II), (c) LSV curves and (d) Tafel slopes of the catalysts. (Pt/C loading: 40 $\mu g_{Pt}/cm^2$)

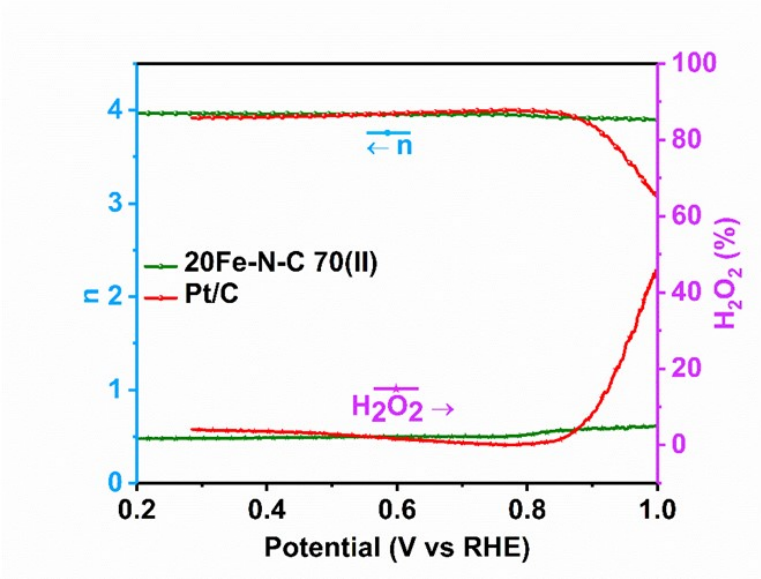

Fig. S24 RRDE result of the catalysts in 0.5M H_2SO_4

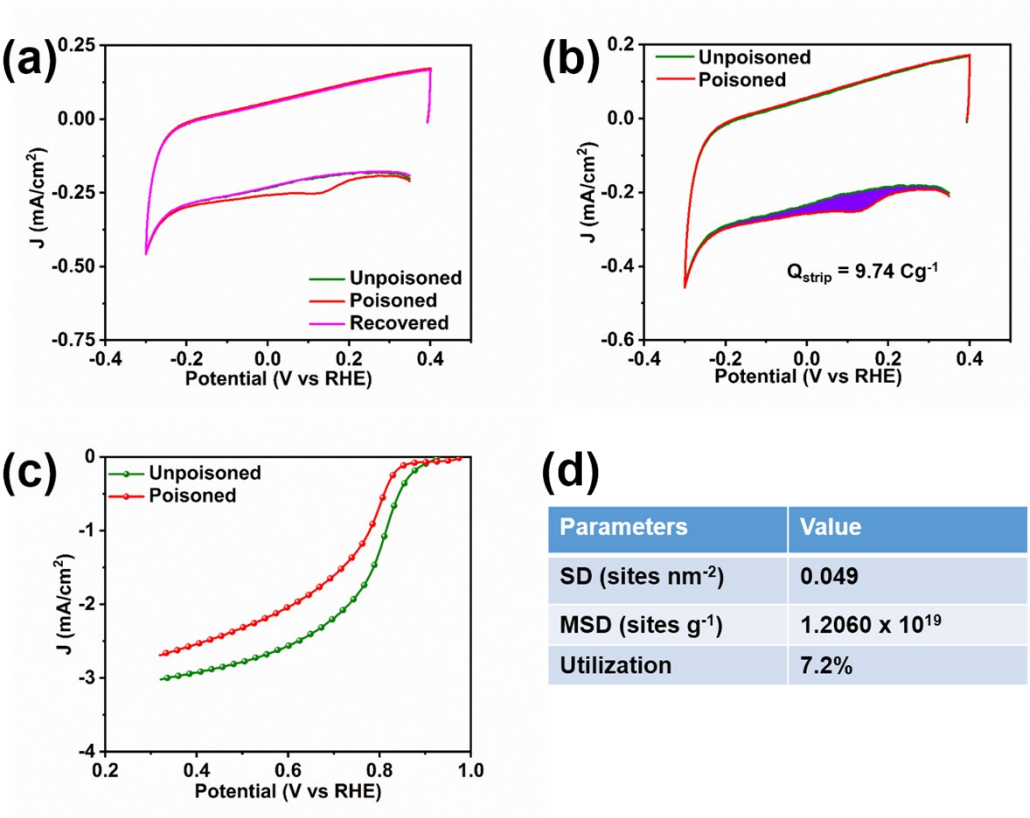

Parameters	Value
SD (sites nm^{-2})	0.049
MSD (sites g^{-1})	1.2060 x 10^{19}
Utilization	7.2%

Fig. S25 Site density evaluation of 20Fe-N-C 70(II) showing (a) Nitrite stripping voltammetry in N_2-saturated 0.5 M acetate electrolyte buffer (pH 5.2) before, during and after nitrite adsorption (b) CV curves in the reductive stripping region (c) ORR performance of catalyst layer before and after nitrite adsorption (d) SD calculation.

Table S5. Review of ORR activity of highly active Fe single-atom catalysts in 0.1 M KOH reported in recent literature.

[a]: 1 M KOH, [b]: 0.1 M NaOH

Catalyst	Fe Content	Loading ($\mu g/cm^2$)	E_{on} & $E_{1/2}$	Tafel Slope (mV/dec)	Ref.
20Fe-N-C 70(II)	**1.55 wt%**	**400**	**E_{on}: 0.988 V vs RHE** **$E_{1/2}$: 0.903 V vs RHE**	**32**	**This work**
Fe–N–C	-	200	$E_{1/2}$: 0.846 V vs RHE	-	[1]
Fe-N/P-C-700	1.03 at%	600	E_{on}: 0.941 V vs RHE $E_{1/2}$: 0.867 V vs RHE	-	[2]
Fe-NC SAC	8.9 wt%	600	E_{on}: 0.98 V vs RHE $E_{1/2}$: 0.90 V vs RHE	48	[3]
Fe0.5-N-C	0.5 wt%	274	$E_{1/2}$: 0.92 V vs RHE	-	[4]
SC-Fe	0.23 at%	250	$E_{1/2}$: 0.869 V vs RHE	51.3	[5]
Fe-N-C-800	1.09 wt%	459	$E_{1/2}$: 0.883 V vs RHE	78.41	[6]
Fe_{SA}-N-C	1.76 wt%	280	E_{on}: 1.00 V vs RHE $E_{1/2}$: 0.891 V vs RHE	-	[7]
Fe-SAs/NPS-HC	0.48 at%	-	$E_{1/2}$: 0.912 V vs RHE	36	[8]
Fe-N-DSC	0.8 at%	102	E_{on}: 1.03 V vs RHE $E_{1/2}$: 0.84 V vs RHE	-	[9]
FeCl1N4/CNS	1.5 wt%	501	$E_{1/2}$: 0.921 V vs RHE	51	[10]
Fe-ISAs/CN	2.16 wt%	408	E_{on}: 0.986 V vs RHE $E_{1/2}$: 0.900 V vs RHE	52	[11]
S,N-Fe/N/C-CNT	0.8 at%	600	E_{on}: 0.96 V vs RHE $E_{1/2}$: 0.85 V vs RHE	-	[12]
26AMP-in	-	600	$E_{1/2}$: 0.89 V vs RHE	71.5	[13][a]
Fe-CB@PAN-1000	0.13 at%	800	$E_{1/2}$: 0.884 V vs RHE	-	[14][b]
Fe-N-C	0.5 at%	620	E_{on}: 1.08 V vs RHE $E_{1/2}$: 0.88 V vs RHE	-	[15][b]

References:

[1] Nature Energy 6, 834–843 (2021).

[2] Journal of the American Chemical Society 2020, 142, 5, 2404–2412.

[3] Nature Communications 2019, 10, 1278.

[4] Journal of the American Chemical Society 2019, 141, 2035.

[5] Angewandte Chemie International Edition 2019, 58, 4963.

[6] Journal of Materials Chemistry A 2019, 7, 11007.

[7] Angewandte Chemie International Edition 2018, 57, 8525.

[8] Nature Communications 2018, 9, 5422.

[9] ACS Nano 2018, 12, 208.

[10] Energy & Environmental Science 2018, 11, 2348.

[11] Angewandte Chemie International Edition 2017, 56, 6937.

[12] Angewandte Chemie International Edition 2017, 56, 610.

[13] Nano Energy 38 (2017) 201-209.

[14] Journal of Colloid and Interface Science 502 (2017) 44-51.

[15] Chinese Journal of Catalysis 37 (2016) 539–548.